

Accepted Manuscript

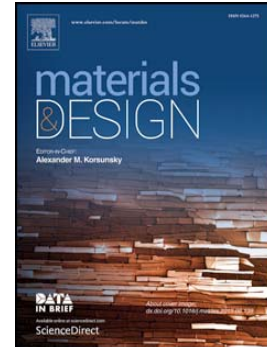
Effect of pitch difference between the bolt–nut connections upon the anti-loosening performance and fatigue life

Nao-Aki Noda, Xin Chen, Yoshikazu Sano, Magd Abdel Wahab, Hikaru Maruyama, Ryota Fujisawa, Yasushi Takase

PII: S0264-1275(16)30128-9
DOI: doi: [10.1016/j.matdes.2016.01.128](https://doi.org/10.1016/j.matdes.2016.01.128)
Reference: JMADE 1329

To appear in:

Received date: 22 November 2015
Revised date: 27 December 2015
Accepted date: 27 January 2016



Please cite this article as: Nao-Aki Noda, Xin Chen, Yoshikazu Sano, Magd Abdel Wahab, Hikaru Maruyama, Ryota Fujisawa, Yasushi Takase, Effect of pitch difference between the bolt–nut connections upon the anti-loosening performance and fatigue life, (2016), doi: [10.1016/j.matdes.2016.01.128](https://doi.org/10.1016/j.matdes.2016.01.128)

This is a PDF file of an unedited manuscript that has been accepted for publication. As a service to our customers we are providing this early version of the manuscript. The manuscript will undergo copyediting, typesetting, and review of the resulting proof before it is published in its final form. Please note that during the production process errors may be discovered which could affect the content, and all legal disclaimers that apply to the journal pertain.

Effect of Pitch Difference between the Bolt-Nut Connections upon the Anti-Loosening Performance and Fatigue Life

Nao-Aki Noda^{a*}, Xin Chen^{a,b}, Yoshikazu Sano^a, Magd Abdel Wahab^b,
Hikaru Maruyama^a, Ryota Fujisawa^a, Yasushi Takase^a

^a*Department of Mechanical Engineering, Kyushu Institute of Technology, Kitakyushu 804-8550, Japan*

^b*Department of Mechanical Construction and Production, Faculty of Engineering and Architecture, Ghent University, 9000 Ghent, Belgium*

*Corresponding author: noda@mech.kyutech.ac.jp

Abstract

In this paper, the effect of a slight pitch difference between a bolt and nut is studied. Firstly, by varying the pitch difference, the prevailing torque required for the nut rotation, before the nut touches the clamped body, is measured experimentally. Secondly, the tightening torque is determined as a function of the axial force of the bolt after the nut touches the clamped body. The results show that a large value of pitch difference may provide large prevailing torque that causes an anti-loosening effect although a very large pitch difference may deteriorate the bolt axial force under a certain tightening torque. Thirdly, a suitable pitch difference is determined taking into account the anti-loosening and clamping abilities. Fourthly, fatigue experiments are conducted using three different values of pitch difference for various stress amplitudes. It is found that the fatigue life could be extended when a suitable pitch difference is considered. Furthermore, the chamfered corners at nut ends are considered, and it is found that the finite element analysis with considering the chamfered nut threads has a good agreement with the experimental observation. Finally, the most desirable pitch difference required for improving both anti-loosening and fatigue life is proposed.

Keywords: Bolt-nut connection, Pitch difference, Anti-loosening performance, Fatigue life,

Finite element method

1 Introduction

The bolt-nut connections are important joining elements and are widely used to connect and disconnect members conveniently at a low cost. Reference [1] fully reviewed the history as well as the evolution of the screw fasteners. To ensure that structures are safety joined, good anti-loosening performance and high fatigue strength are required. Most previous studies have been mainly focusing on anti-loosening performance [2-7], and few studies have contributed to improvements in the fatigue strength [8-17]. This is because a high stress concentration factor, e.g. $K_t=3-5$, appears at the No.1 bolt thread and it is not easy to reduce it. Moreover, usually for special bolt-nut connections the anti-loosening ability affects the fatigue strength and the cost significantly. In other words, anti-loosening bolt-nut connections have not been developed until now without a reduction in fatigue strength and a raising in the cost.

This paper, therefore, focuses on the effect of pitch difference in a connection on the anti-loosening performance and fatigue life. As shown in Fig. 1, if the nut pitch is larger than the bolt pitch, the thread No. 1 at the left-hand side is in contact before the loading and becomes in no-contact status after the loading as shown in Fig. 1 (a). However, if the nut pitch is smaller than the bolt pitch, the thread No.1 at the right-hand side is in contact before the loading and remains in contact after loading, also the contact force becomes larger after the loading as shown in Fig. 1 (b). Therefore, the largest stress concentration at thread No.1 can be reduced only by a larger nut pitch.

The concept of differential pitch was first suggested by Stromeyer [18] in 1918. He suggested that the load distribution in a threaded connection thread could be optimized by varying the relative pitches. Then, the theoretical load distribution in bolt-nut has been developed by Sopwith [19], who also used his formula to discuss the load distribution improvement along the bolt threads by varying pitch. He found that a smaller

pitch in the bolt than in the nut would improve the load distribution. Sparling [20] found that the fatigue strength of the bolt can be improved by increasing the clearance between the first few engaged threads at the load bearing face of the nut by tapering the nut thread, which produces an effective difference in pitch. This modification was investigated by Kenny and Patterson [21, 22] by applying the frozen stress three-dimensional photoelasticity. Maruyama [23] analyzed the influence of pitch error and the loaded flank angle error of the bolt thread upon the stress at the root of the bolt thread by copper-electroplating method with the finite element method. It was considered that the pitch adjustment has a larger effect than the flank angle adjustment for improving the fatigue strength of the bolt thread.

However, the previous studies on pitch difference were limited to fatigue strength improvement, and the effect of pitch difference on the anti-loosening performance has not been investigated yet. There is no systematic experimental data are available, e.g. the $S-N$ curves for specimens of different pitch differences have not been obtained.

Table 1 shows a comparison of some special bolt-nut connections. Most of the special bolt-nuts have either more components or very special geometry, leading to a complex manufacture process and a high cost which is usually more than 3 times of the normal bolt-nut. The suggested nut in this study can be manufactured as the same way as the normal nut, and the cost is predicted to be about 1.5 times of the normal nut considering the modification of thread tap as well as the checking procedure on the pitch difference.

Our previous experimental work clarified that the fatigue life is improved by introducing a suitable pitch difference under a certain level of stress amplitude [24, 25]. In this study, at first, the effect of pitch difference on the anti-loosening performance will be studied experimentally, and the most desirable pitch difference will be proposed taking into account the effect on clamping ability. Furthermore, the fatigue experiments

will be carried out to investigate the effect of pitch difference on the improvement of fatigue life. The finite element analysis will also be applied to discuss the stress status at bolt thread. Taking the anti-loosening performance and the fatigue life improvement into account, the most desirable pitch difference will be proposed.

2 Effect of the Pitch Difference on the Nut Rotation

2.1 Bolt-Nut Specimens

Japanese Industrial Standard (JIS) M16 bolt-nut connections were employed to study the effect of a slight pitch difference. Figure 2 shows the dimensions of bolt-nut specimen used in this study. Figure 3 shows a schematic illustration of bolt-nut connection having pitch differences. Usually, standard M16 bolts and nuts have the same pitch of 2 mm, but herein the nut pitch is slightly larger than the bolt pitch. The clearance between the bolt-nut threads is equal to 125 μm . The bolt material was chromium-molybdenum steel SCM435 (JIS), and the nut material was medium carbon steel S45C (JIS) quenched and tempered, whose properties are indicated in Table 2, and whose stress-strain curves are shown in Fig. 4, respectively.

Figure 3 (a) also shows a contact status between bolt and nut threads during the tightening process. As the nut is screwed onto the bolt, the pitch difference is accumulated. Finally, the first and sixth nut threads become in contact with the bolt threads as shown in Fig. 3 (a). The distance, δ_t , where the contact takes place, can be obtained geometrically using Equations (1) and (2).

$$n_c \alpha = 2C_x, C_x = \frac{C_y}{\tan \theta'} \quad (1)$$

$$\delta_t = n_c p \quad (2)$$

where p is the pitch of bolt (2 mm), α is the pitch difference, n_c is the number of nut thread in contact except for $n=1$, θ is the thread angle ($=60^\circ$), $\theta' = (\pi - \theta) / 2$, and C_x

and C_y are the horizontal and vertical clearances between bolt and nut as shown in Fig. 3 (b). The specimens in this study had five different levels of pitch difference α , namely $\alpha=0$ (for standard connection), α_{small} , α_{middle} , α_{large} and $\alpha_{verylarge}$. Herein, it should be noted that the nut has 8 threads and therefore Equation (1) is valid when n_c is less than 8. Table 3 shows the distance, δ_t , and nut thread number in contact, n_c , obtained from Equations (1) and (2). The distance, δ_t , can be predicted for α_{middle} , α_{large} and $\alpha_{verylarge}$, although no thread contact may be expected for α_{small} , because n_c is larger than the total number of threads number 8 for the nut.

2.2 Prevailing Torque

After the nut threads become in contact over distance δ_t as shown in Fig. 3 (a), the so-called prevailing torque is required for the nut rotation even though the nut does not touch the clamped body yet. Table 3 also lists the prevailing torque T_p measured by using an electric torque wrench.

For $\alpha=\alpha_{small}$, the value of n_c is larger than 8, and therefore all threads are in non-contact status and the prevailing torque was zero experimentally. For $\alpha=\alpha_{middle}$, since value n_c is smaller than 8, the threads are in contact and prevailing torque was $T_p=25$ N·m. For $\alpha=\alpha_{large}$, prevailing torque was $T_p=50$ N·m, and for $\alpha=\alpha_{verylarge}$ the threads deformed largely and the nut was locked before touching the clamped body since it cannot be rotated anymore.

2.3 Prevailing Torque vs Clamping Force

Since the bolt and nut are used for connecting components or structures, the clamping ability to produce enough bolt-axial force is essential. Therefore, after the nut touches the clamped body, the relationship between the tightening torque and the clamping force was investigated. Note that tightening torque T is different from prevailing torque T_p ,

which is defined only before the nut touches the clamped body. To obtain the relationship between torque and clamping force, the torque was controlled by using an electric torque wrench, and the clamping force was measured by using the strain gauge attached to the clamped body surface as shown in Fig. 5 (a). The uniaxial strain gauge with a length of 2 mm KFG-2 (Kyowa Electronic Instruments Co., Ltd.) was used in this measurement. Before the experiments, calibration tests were performed by compressing the clamped body to obtain the relationship between the clamping force and surface strain as shown in Fig. 5 (a). Similar tests were performed to calibrate the torque wrench as shown in Fig. 5 (b). In order to compare anti-loosening performance for different pitch differences, the same tightening torque was applied. When the tightening torque of 70 N·m was applied to the standard bolt-nut ($\alpha=0$), the bolt-axial force became 24 kN. The bolt axial force 24 kN is rather smaller compared to the normal bolt-axial force as the standard bolt-axial force 59.3 kN recommended in [26]. However, if a larger bolt-axial force is used, the effect of α on the anti-loosening performance cannot be clearly demonstrated because the bolt-nut seizure occurs. In fact, when a torque of 150 N·m was applied in our preliminary experiments, bolt-nut seizure was sometimes observed even for $\alpha=0$ and $\alpha=\alpha_{small}$. This is because in this study, turning was used for manufacturing nuts, which leads to the bolt-nut seizure occurring more easily than tapping, which is usually used for manufacturing nuts. The tapping was not used in this study because of the high cost. However, in the further research, the tapping nut can be used to prevent the bolt-nut seizure. In this study, therefore, the smaller tightening torque of 70 N·m is used to compare the anti-loosening ability conveniently.

Figure 6 shows the tightening torque vs. clamping force as experimentally obtained. When $\alpha=\alpha_{small}$, the torque-clamping force relationship was same with the one of $\alpha=0$.

When $\alpha=\alpha_{middle}$, the prevailing torque of 25 N·m was required before the nut touches the clamped plate. Under the same tightening torque of 70 N·m, the clamping force was reduced to 20 kN. When $\alpha=\alpha_{large}$, under a torque of 70 N·m the axial force decreased significantly to 8 kN, which was only 1/3 of the axial force of $\alpha=0$.

3 Loosening Experiment

3.1 Device

Based on the torque-axial force relationship obtained above, the loosening experiments were performed to investigate the effect of pitch difference on the anti-loosening performance. For each pitch difference α , two specimens were tested. As shown in Fig. 7, the experimental device was an impact-vibration testing machine based on NAS3350 (National Aerospace Standard), whose vibration frequency was about 30 Hz, and vibration acceleration is 20 g. The maximum vibration cycle of NAS3350 is 30 000, therefore, if the number of vibration cycles was over 30 000, the anti-loosening performance may be considered to be good enough. A counter connected with the experimental device shows the number of cycles of vibrations. As states in Section 2.3, the bolt-axial force 24 kN was considered for the standard bolt-nut, and the corresponding tightening torque was 70 N·m. In order to compare the anti-loosening performance under the same condition, in this paper, the nuts were tightened to the same torque of 70 N·m for all the specimens.

3.2 Results

Table 4 lists the number of cycles for the start loosening and the nut dropping. Table 4 also lists the prevailing torque measured in the loosening experiments and the bolt axial forces estimated from Fig. 6. For $\alpha=0$ and $\alpha=\alpha_{small}$, the nuts dropped at about 1,000

cycles. For $\alpha=\alpha_{middle}$, the nuts did not drop until 30 000 cycles, but the loosening was observed for one specimen. For $\alpha=\alpha_{large}$, no loosening was observed until 30 000 cycles although the axial force was estimated to be only 8 kN. It may be concluded that if α is too small, the anti-loosening cannot be expected and if α is too large, the clamping ability is not good enough. By considering both the anti-loosening and clamping abilities, $\alpha=\alpha_{middle}$ can be selected as the most suitable pitch difference. It should be noted that the most desirable pitch difference of $\alpha=\alpha_{middle}$ was obtained with a clearance of $C_y=125\ \mu\text{m}$.

4 Finite Element Analysis

The previous discussion shows that $\alpha=\alpha_{large}$ has a good anti-loosening performance but insufficient clamping ability. This is due to the large deformation of the threads during the tightening process. To confirm this, an axisymmetric model of the bolt-nut connection was constructed by using the FEM code MSC.Marc/Mentat 2012. The material of the bolt was SCM435 and the material of the nut was S45C to match the experimental conditions. These stress-strain curves are indicated in Fig. 4. Herein, bolt, nut and clamped body are modeled as three bodies in contact. In the tightening process, the accumulated pitch difference causes the axial force between the bolt threads engaged with the nut thread. In this modelling, the bolt head is fixed in the horizontal direction, and the tightening process is expressed by shifting the nut threads position discontinuously, one by one, at the pitch interval. As the nut is moving towards the bolt head, the accumulation of the pitch difference leads to a slight overlap between the bolt threads and the nut threads. The direct constraints method is invoked in the detection of contact in MSC. Marc [27], then, the nut is compressed while the bolt is stretched in the simulation. In this way, the axial force between the bolt threads can be investigated step by step as the nut is shifted onto the bolt. It should be noted that this axisymmetric

simulation may include some numerical errors but the real axial force between the bolt threads is difficult to be measured experimentally because the nut is engaged at this position. The multifrontal sparse solver was used. The isotropic hardening law was assumed with von Mises yield criterion. Friction coefficient of 0.3 was assumed and Coulomb friction was used. In the next sub-section, the results for $\alpha=\alpha_{middle}$ and $\alpha=\alpha_{verylarge}$ will be compared.

4.1 Bolt Axial Force

Since the nut pitch is larger than the bolt pitch, a bolt axial force, F_α , in tension appears between the bolt threads. F_α corresponds to prevailing torque T_p . It should be noted that F_α is different from the bolt axial force (clamping force) obtained in Fig. 6. Here, the axial force F_α between bolt threads arising from the accumulation of pitch difference in the tightening process. Figure 8 (a) indicates F_α for $\alpha=\alpha_{middle}$ before the nut touches the clamped body from Position A to Position G. Position A is where the prevailing torque appears, and Position B is where the nut thread shifted at the pitch interval from Position A and so on. Finally, Position G is where the nut starts contacting the clamped body. From Position A to Positions B, C, the whole nut is being shifted onto the bolt, and therefore the accumulated pitch difference affects the results. From Position C to Positions D, E, F, G, the pitch difference is not accumulated since the whole nut is already in contact with the bolt.

Figure 8 (b) shows F_α for $\alpha=\alpha_{verylarge}$ from Position A to Position H. Position A is where the prevailing torque appears, and Position H is where the nut starts contacting the clamped body. In contrast to the case of $\alpha=\alpha_{middle}$, as the nut is being shifted onto the bolt, the bolt axial forces corresponding to nut threads No.1 and No.8 become smaller than that in the middle part. This result is due to nut threads No.2 and No.7, which are

also in contact as well as threads No.1 and No.8. Under $\alpha=\alpha_{middle}$ only nut threads No.1 and No.8 are in contact with bolt threads.

4.2 Plastic Deformation

Figure 9 (a) shows the equivalent plastic strain of threads for $\alpha=\alpha_{middle}$ at Position G. Similarly, Fig. 9 (b) shows the equivalent plastic strain of threads for $\alpha=\alpha_{verylarge}$ at Position H. It may be concluded that too large pitch difference $\alpha=\alpha_{verylarge}$ may cause the large deformation at nut threads resulting in deterioration of bolt clamping ability. A suitable pitch difference may cause the reasonable deformation and may not reduce the clamping force.

5 Effect of the Pitch Difference on the Fatigue Strength

5.1 Results and Discussion

Our previous experiments clarified that the fatigue life was improved by introducing a pitch difference $\alpha=\alpha_{small}$ under a certain level of stress amplitude [24-25]. According to the loosening experiments, it was found that $\alpha=\alpha_{middle}$ was the most desirable pitch difference to realize the anti-loosening performance. To improve the fatigue life as well as the anti-loosening performance, fatigue experiments were conducted systematically for three types of specimens, i.e. $\alpha=0$, $\alpha=\alpha_{small}$ and $\alpha=\alpha_{middle}$ with various levels of stress amplitude.

The 392 kN Servo Fatigue Testing Machine with a frequency of 8 Hz was used in this study. The pulsating tension fatigue experiments with a stress ratio of $R=0.14-0.56$ were conducted under a fixed average stress of $\sigma_m=213$ MPa. Figure 10 shows the obtained $S-N$ curves. Independent of α , it was found that the fatigue limit at $N=2\times 10^6$ cycles was 60 MPa.

The fractured specimens were first investigated. As an example, Fig. 11 shows longitudinal sections for $\alpha=0$, $\alpha=\alpha_{small}$ and $\alpha=\alpha_{middle}$, when the stress amplitude $\sigma_a=100$ MPa. For $\alpha=0$, the initial crack may occur at thread No.2, and final fracture happened at thread No.1. For $\alpha=\alpha_{small}$ and $\alpha=\alpha_{middle}$, long cracks were observed at threads No.5 and No.6, and therefore initial crack may occur at threads No.5 or No.6 extending towards thread No.1. Moreover, when the stress amplitude was $\sigma_a=60$ MPa, the fractured specimens of $\alpha=\alpha_{small}$ and $\alpha=\alpha_{middle}$ also showed more than 1 mm long cracks initiating from the thread surface although no long crack was observed for $\alpha=0$. Therefore, the actual fatigue limit of the bolt specimen may be lower than 60 MPa for $\alpha=\alpha_{small}$ and $\alpha=\alpha_{middle}$.

Figure 12 shows the crack initiation and extension mechanism for $\alpha=\alpha_{small}$ and $\alpha=\alpha_{middle}$. As shown in Fig.12 (a), crack initiated at thread No.6. After the crack extended at No.6, the distributed load F_6 became smaller and F_5 became larger as shown in Fig. 12 (b), $F'_5 > F'_6$. Then, a new crack initiated at thread No.5 as show in Fig.12 (c). By extending new cracks from No.6 toward No.1, the final fracture happened nearby No.1. In this way, since many cracks initiated and propagated one by one, the fatigue life of $\alpha=\alpha_{small}$ and $\alpha=\alpha_{middle}$ can be extended compared with the one of $\alpha=0$.

The experimental observation in Fig.11 shows that the crack initiated around the root of bolt thread $\psi=-60^\circ\sim 60^\circ$, instead of the nut thread contact region. Therefore, in this study, the contact fatigue concept was not considered.

When the stress amplitude was larger than 80 MPa, as shown in Fig. 10, the fatigue life for $\alpha=\alpha_{small}$ was about 1.5 times larger than that of $\alpha=0$. Also, the fatigue life for $\alpha=\alpha_{middle}$ was about 1.2 times larger than that of $\alpha=0$. The results showed that the most desirable pitch difference $\alpha=\alpha_{small}$ for fatigue performance was different from the most desirable pitch difference of $\alpha=\alpha_{middle}$ for anti-loosening performance.

In Fig.10, there are different fatigue data between $\alpha=\alpha_{small}$ and $\alpha=0$ because the stress status at bolt thread changed when $\alpha=\alpha_{small}$ was introduced. On the other hand, as shown in Fig.6, since there was no prevailing torque appears in the tightening process for $\alpha=\alpha_{small}$, it has the same torque-axial force relationship with the normal specimen $\alpha=0$. The effect of pitch difference on the fatigue life is different from the effect on tightening process. This is because that the fatigue damage is mainly controlled by the stress amplitude produced by the axial loading at the bolt threads.

5.2 Strength Analysis

To clarify the effect of the pitch difference on the stress at the bolt threads, the elastic-plastic FE analyses were performed for $\alpha=0$ and $\alpha=\alpha_{small}$ under load $F=30\pm 14.1$ kN. The axisymmetric finite element model of bolt-nut connection is shown in Fig. 13. A cylindrical clamped plate was modeled with an inner diameter of 17.5 mm, outer diameter of 50 mm and thickness of 35 mm. The material of the bolt and clamped body was SCM435 and the material of the nut was S45C to match the experimental conditions. These stress-strain curves are indicated in Fig. 4. The bolt, nut and clamped body were modeled as three contact bodies. A fine mesh was created at the root of bolt thread with the size of $0.015\text{mm}\times 0.01\text{mm}$, and 4-noded, axisymmetric solid, full integration element was used. The isotropic hardening law was assumed with von Mises yield criterion. Friction coefficient of 0.3 with Coulomb friction was used for the analysis. The clamped body was fixed in the horizontal direction, and cyclic load $F=30\pm 14.1$ kN was applied on the bolt head as shown in Fig. 13. Then, the stress status under the maximum load $F=30+14.1$ kN and the minimum load $F=30-14.1$ kN was considered to obtain the endurance limit diagrams. Figure 14 defines the angle ψ at the bolt thread. In the FE analysis $\sigma_{\psi\max}$ was the stress σ_{ψ} at each thread under the maximum

load, and $\sigma_{\psi\min}$ was the stress σ_{ψ} at each thread under the minimum load. The stress amplitude and mean stress were investigated at the same angle ψ where the maximum stress amplitude appears, since the stress amplitude is the most important parameter for fatigue analysis. The mean stress σ_m and stress amplitude σ_a at each thread are defined as follows:

$$\sigma_m = \frac{\sigma_{\psi\max} + \sigma_{\psi\min}}{2}, \quad \sigma_a = \frac{\sigma_{\psi\max} - \sigma_{\psi\min}}{2} \quad (3)$$

The maximum stress amplitude and the mean stress at each bolt thread are plotted in Fig. 15 and compared with Soderberg line representing the endurance limit for plain specimen. Figure 15 indicates that the stress amplitude at thread No.1 for $\alpha=\alpha_{small}$ is much smaller than that of $\alpha=0$ although the stress amplitudes of threads No.4 to No.8 are much larger than those of $\alpha=0$. Therefore, the cracks may appear faster at No.4 to No.8 for $\alpha=\alpha_{small}$, but the fatigue life time is extended as shown in Fig. 10 since the crack propagation from threads No.8 to No.1 needs longer time.

6 Effect of incomplete nut thread

In the above discussion, the complete thread model of 8-thread-nuts were considered by FE analyses, but usually as shown in Fig. 16 (a) both ends of nuts have chamfered corners, which are required to make bolt inserted smoothly. This types of nuts were used in the fatigue experiments. Therefore, the chamfered corner was modeled first by an incomplete thread model A as shown in Fig. 16 (b). Figure 17 shows FE mesh for model A and the endurance limit diagram, when $\alpha=\alpha_{small}$ and $\sigma_a=100$ MPa. From Fig. 17 (b), it can be seen that the stress in thread No.8 decreases and the stress in thread No.6 increases. However, the stress in thread No.6 is not the most dangerous because thread No.8 is still in contact with a nut thread.

Therefore, thread model B as shown in Fig. 16 (c) is considered, where the incomplete nut thread does not contact bolt thread anymore due to the chamfered nut-ends. Figure 18 (a) shows the FE mesh for model B. Figure 18 (b) (c) show the maximum and minimum stresses in each thread when the maximum and minimum load $F=30\pm 14.1$ kN are applied. When $\alpha=0$, the maximum stress amplitude appears at thread No.2. Therefore, the analytical result coincides with the experimental result in Fig. 11 (a). When $\alpha=\alpha_{small}$, the maximum stress amplitude appears at thread No.6, which is close to the crack location in Fig. 11 (b).

Figure 18 (d) (e) show the endurance limit diagrams for $\alpha=0$ and $\alpha=\alpha_{small}$. By changing 8-thread-model to 6-thread-model B, the most dangerous thread for $\alpha=0$ is changed from thread No.1 to thread No.2. For $\alpha=\alpha_{small}$, thread No.6 becomes the most dangerous, corresponding to Fig. 11 (b). It is seen that the 6-thread-model B is useful to consider the chamfered nut threads at both ends in order to explain the experimental results.

One may think that replicating the actual geometry of chamfered threads in Fig. 16 (a) should be used in the FE model. However, the chamfered angle is not always the same. And the difference between the results for model B and the chamfered model with actual geometry is not very large for $\alpha=\alpha_{small}$ because threads No.1 and No.8 are not in contact. Only the largest difference appears at thread No. 1 for $\alpha=0$ because for model B there are no threads in contact at No.1 thread. In this study, therefore, simple incomplete thread model B has been used because our main target is to analyze the model having pitch difference α . The results of the chamfered model for standard bolt-nut $\alpha=0$ are indicated in appendix A.

7 Suitable Pitch Difference

The main goal of this study is to find out a suitable pitch difference in order to improve both anti-loosening effect and fatigue life. Figure 19 shows a schematic illustration of the fatigue life improvement and anti-loosening improvement by varying the pitch difference when the results of $\alpha=0$ are regarded as the reference level. On one hand, to improve the fatigue life, the most desirable pitch difference may be close to α_{small} as shown in Fig. 10. On the other hand, to improve the anti-loosening performance, the most desirable pitch difference should be larger than α_{middle} and close to α_{large} as shown in Table 4, although the nut locking phenomenon may happen if α is over $\alpha_{\text{verylarge}}$. Therefore, a suitable range for α can be indicated as shown in Fig. 19.

In this study, the bolt material SCM435 and nut material S45C are assumed. The stress-strain curves are indicated in Fig. 4. This design can be applied to bolt-nut connections made in other materials which have suitable elastic-plastic properties since the plastic deformation is required in order to realize the anti-loosening performance.

8 Conclusions

In this study, a slight pitch difference α was considered for the M16 bolt-nut connections. The loosening experiments as well as the fatigue experiments were conducted under different pitch differences. Finite element analysis was used to investigate the stress and deformation at the bolt threads and the fatigue strength. The conclusions can be summarized as follows:

- (1) Considering both the anti-loosening performance and the clamping ability, $\alpha=\alpha_{\text{middle}}$ is found to be the most desirable pitch difference. This is because the nuts did not drop for $\alpha=\alpha_{\text{middle}}$ without losing clamping ability.
- (2) The anti-loosening experiments show that the nuts did not drop for $\alpha=\alpha_{\text{large}}$, but

clamping ability is deteriorated. FEA shows that for $\alpha=\alpha_{verylarge}$, the large plastic deformation happens at threads of nut.

(3) It is found that $\alpha=\alpha_{small}$ is the most desirable pitch difference to extend the fatigue life of the bolt-nut connection. Compared with the standard bolt-nut connection, the fatigue life for $\alpha=\alpha_{small}$ can be extended to about 1.5 times.

(4) The 6-thread-model as shown in Fig. 18 is useful for analyzing 8-thread-nut model because nuts always have chamfered threads at both ends. Then, the results are in good agreement with the experimental results.

(5) A suitable pitch difference to improve both anti-loosening and fatigue life can be illustrated as shown in Fig. 19.

The errors and uncertainties associated with the measurements or predictions are always of concern in a study of this nature. In the loosening experiment, two specimens with the same pitch difference were tested together in order to avoid the uncertainties. In the fatigue experiment in Fig. 10, the $S-N$ curves may have variations but they are distinct depending on the pitch difference. In the axisymmetric FE modelling may have some errors but previously one of the authors have compared the load distributions in bolt threads between the axisymmetric modelling and the three-dimensional modelling. Then, the relative errors between the two models are found to be less than 12% [28].

Appendix A: The results for chamfered model

Figure A1 shows the chamfered model replicating the actual geometry in Fig. 16 (a). Figure A2 shows the results of the chamfered model in comparison with the results of the complete thread model in Fig. 13 when $\alpha=0$. It is seen that because of no contact at thread No.8 in the chamfered model, mean stress σ_m and stress amplitude σ_a increase except at thread No.1. Since the rigidity of nut thread No.1 decreases in the chamfered

model, the stress at bolt thread No.1 does not change very much.

Acknowledgments

The authors wish to express their thanks to the member of their group, Mr. Yu-Ichiro Akaishi and Mr. Yang Yu for their assistance in this study. The authors acknowledge the international collaboration grant funded by Commissie Wetenschappelijk Onderzoek (CWO), Faculty of Engineering and Architecture, Ghent University. The research for this paper was financially supported by the Japanese Ministry of Education research expenses [grant number 23560164]; and Kitakyushu Foundation for the Advancement of Industry Science and Technology.

References


- [1] Bhattacharya, A., Sen, A., and Das, S., An Investigation on the Anti-Loosening Characteristics of Threaded Fasteners under Vibratory Conditions, *Mechanism and Machine Theory*, 2010; 45, pp. 1215-1225. DOI: 10.1016/j.mechmachtheory.2008.08.004.
- [2] Hard Lock Kogyo KK, Hard Lock Nut, Japan Patent 2002–195236, 2002 (In Japanese).
- [3] Izumi, S., Yokoyama, T., Iwasaki, A., and Sakai, S., Three-Dimensional Finite Element Analysis of Tightening and Loosening Mechanism of Threaded Fastener, *Engineering Failure Analysis*, 2005; 12(4), pp. 604-615. DOI: 10.1016/j.engfailanal.2004.09.009.
- [4] Izumi, S., Yokoyama, T., Teraoka, T., Iwasaki, A., Sakai, S., Saito, K., Nagawa, M., and Noda, H., Verification of Anti-loosening Performance of Super Slit Nut by Finite Element Method, *Transaction of the Japan Society of Mechanical Engineers*, 2005; 703(71), pp. 380-386, (in Japanese).

- [5] Chen, D. H., Shimizu, E., and Masuda, K., Relation between Thread Deformation and Anti-Loosening Effect for Nut with Circumference Slits, *Transaction of the Japan Society of Mechanical Engineers*, 2012; 788(78), pp. 390-402. DOI: 10.1299/kikaia.78.390.
- [6] Noda, N.-A., Xiao, Y., and Kuhara M., Optimum Design of Thin Walled Tube on the Mechanical Performance of Super Lock Nut, *Journal of Solid Mechanics and Materials Engineering*, 2008; 2(6), pp. 780-791. DOI: 10.1299/jmmp.2.780.
- [7] Ranjan, B. S. C., Vikranth, H. N., and Ghosal, A., A Novel Prevailing Torque Threaded Fastener and Its Analysis, *ASME Journal of Mechanical Design*, 135(10), 101007, 2013. DOI: 10.1115/1.4024977.
- [8] Nishida, S.-I., Urashima, C., and Tamasaki, H., A New Method for Fatigue Life Improvement of Screws, *European Structural Integrity Society*, 1997; 22, pp. 215-225, DOI: 10.1016/S1566-1369(97)80021-0.
- [9] Nishida, S.-I., Screw Connection Having Improved Fatigue Strength, *United States Patent*, 1980; No. 4,189,975.
- [10] Majzoobi, G. H., Farrahi, G. H., and Habibi, N., Experimental Evaluation of the Effect of Thread Pitch on Fatigue Life of Bolts, *International Journal of Fatigue*, 2005; 27(2), pp. 189-196. DOI: 10.1016/j.ijfatigue.2004.06.011.
- [11] Noda, N.-A., Xiao, Y., and Kuhara M., The Reduction of Stress Concentration by Tapering Threads, *Journal of Solid Mechanics and Materials Engineering*, 2011; 8(5), pp. 397-408. DOI: 10.1299/jmmp.5.397.
- [12] Hirai, K. and Uno, N.: Fatigue Strength of Super High Strength Bolt. *Journal of Structural Engineering*, 2005; 595, pp. 117-122.
- [13] Pedersen, N. L., Overall Bolt Stress Optimization. *The Journal of Strain Analysis for Engineering Design*, 2013; 48(3), pp. 155-165.

- [14] Zhou, W., Zhang, R., Ai, S., He, R., Pei, Y., and Fang, D., Load Distribution in Threads of Porous Metal-ceramic Functionally Graded Composite Joints Subjected to Thermomechanical Loading. *Composite Structures*, 2015; 134, pp. 680-688.
- [15] Li, G., Zhang, C., Hu, H., and Zhang, Y., Optimization Study of C/SiC Threaded Joints. *International Journal of Applied Ceramic Technology*, 2014; 11(2), pp. 289-293.
- [16] Lee, C.-H., Kim, B.-J., and Han, S.-Y., Mechanism for Reducing Stress Concentrations in Bolt-Nut Connectors. *International Journal of Precision Engineering and Manufacturing*, 2014; 15(7), pp. 1337-1343.
- [17] Chakherlou, T. N., Maleki, H. N., Aghdam, A. B., and Abazadeh, B., Effect of Bolt Clamping Force on the Fracture Strength of Mixed Mode Fracture in an Edge Crack with Different Sizes: Experimental and Numerical Investigations. *Materials and Design*, 2013; 45, pp. 430-439.
- [18] Stromeyer, C. E., Stress Distribution in Bolts and Nuts. *Trans Inst. N. A.*, 1918; 60, pp. 112-115.
- [19] Sopwith, D. G., The Distribution of Load in Screw Threads. *Proceedings of the Institution of Mechanical Engineers*, 1948; 159, pp. 373-383.
DOI: 10.1243/PIME_PROC_1948_159_030_02
- [20] Sparling, L. G. M., Improving the Strength of Screw Fasteners. *Chart. Mech. Engrs*, 1982; 29, pp. 58-59.
- [21] Patterson, E. A. and Kenny, B., A Modification to the Theory for the Load Distribution in Conventional Nuts and Bolts, *The Journal of Strain Analysis for Engineering Design*, 1986; 21(1), pp. 17-23. DOI: 10.1243/03093247V211017.
- [22] Kenny, B. and Patterson, E. A., Stress Analysis of Some Nut-bolt Connections with Modifications to the Nut Thread Form, *The Journal of Strain Analysis for Engineering Design*, 1985; 20(1), pp. 35-40. DOI: 10.1243/03093247V201035.

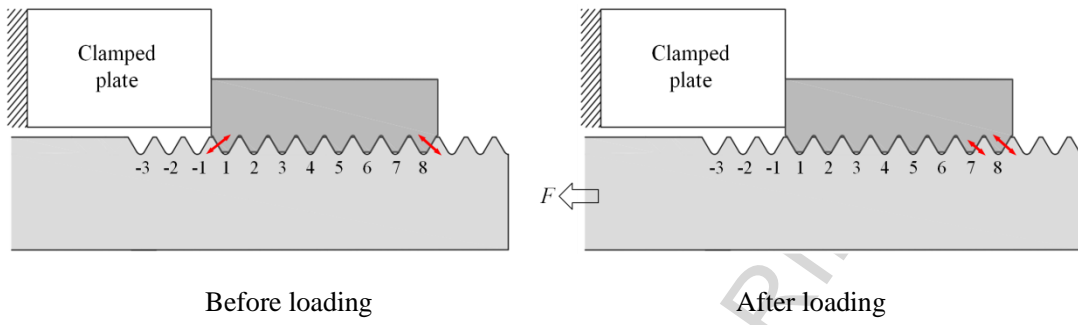
- [23] Maruyama, K., Stress Analysis of a Bolt-Nut Joint by the Finite Element Method and the Copper-Electroplating Method: 3rd Report, Influence of Pitch Error or Flank Angle Error, Transaction of the Japan Society of Mechanical Engineers, 1973; 19(130), pp. 360-368. DOI: 10.1299/jsme1958.19.360.
- [24] Akaishi, Y.-I., Chen, X., Yu, Y., Tamasaki, H., Noda, N.-A., Sano, Y., and Takase, Y., Fatigue Strength Analysis for Bolts and Nuts Which Have Slightly Different Pitches Considering Clearance, Transactions of Society of Automotive Engineers of Japan, 2013; 44(4), pp. 1111-1117, (in Japanese).
- [25] Chen, X., Noda, N.-A., Wahab, M. A., Akaishi, Y.-I., Sano, Y., Takase, Y., and Fekete, G., Fatigue Failure Analysis in Bolt-Nut Connection Having Slight Pitch Difference Using Experiments and Finite Element Method, Acta Polytechnica Hungarica, 2015; 12(8), pp. 61-79.
- [26] Tohnichi torque handbook, Vol.7, Chapter 2 Bolt Tightening, pp. 34-37, (in Japanese).
- [27] Marc 2012, Theory and user information, MSC. Software Corporation, 2012, Vol. A, pp. 540-581.
- [28] Noda, N.-A., Kuhara, M., Xiao, Y., Noma, S., Saito, K., Nagawa, M., Yumoto, A. and Ogasawara, A., Stress Reduction Effect and Anti-loosening Performance of Outer Cap Nut by Finite Element Method, Journal of Solid Mechanics and Materials Engineering, 2008; 2(6), pp. 801-811.

Figure Captions List

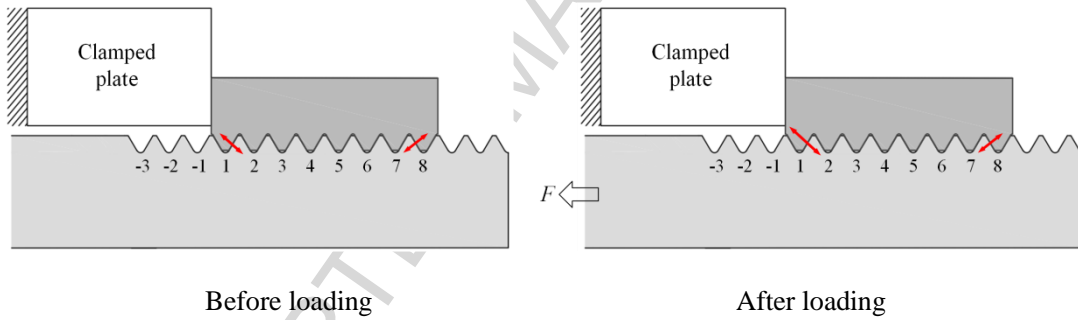
- Fig. 1 Contact status between bolt and nut threads before and after loading ( contact)
- Fig. 2 Bolt-nut specimen (dimensions in mm)
- Fig. 3 Schematic illustration of bolt-nut connection having a pitch difference
- Fig. 4 Stress strain relation for SCM435 (Bolt) and S45C (Nut)
- Fig. 5 (a) Calibration method for bolt axial force measurement and (b) Calibration method for torque wrench
- Fig. 6 Relationship between torque and clamping force
- Fig. 7 Loosening experimental device based on NAS3350 (dimensions in mm)
- Fig. 8 Bolt axial force for the screwing process when the bolt is SCM435 and nut is S45C
- Fig. 9 Equivalent plastic strain when the bolt is SCM435 and nut is S45C
- Fig. 10 $S-N$ curves for $\alpha=0$, α_{small} and α_{middle}
- Fig. 11 Observation of crack trajectories ($\sigma_a=100$ MPa, $F=30\pm 14.1$ kN)
- Fig. 12 Crack initiation and extension mechanism due to thread load
- Fig. 13 Axisymmetric finite element model
- Fig. 14 Local coordinate at the bolt thread
- Fig. 15 Endurance limit diagram ($\sigma_a=100$ MPa)
- Fig. 16 Incomplete threads at nut ends by cut away and incomplete thread models
- Fig. 17 Axisymmetric finite element mesh for model A considering incomplete thread and analytical result

- Fig. 18 Axisymmetric finite element mesh for model B considering incomplete thread and analytical result
- Fig. 19 Schematic illustration of the fatigue life improvement and anti-loosening improvement
- Fig. A1 Axisymmetric finite element mesh for chamfered thread model
- Fig. A2 Comparison between the results of chamfered thread model and complete thread model when $\alpha=0$ and $\sigma_a=100$ MPa

ACCEPTED MANUSCRIPT

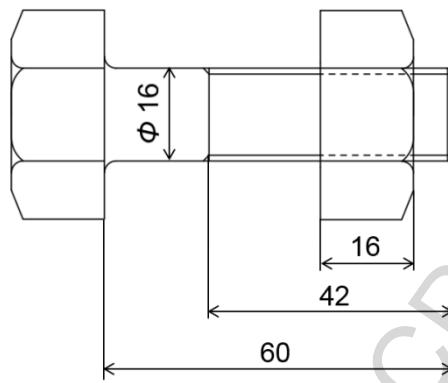


(a) The nut pitch is larger than the bolt pitch

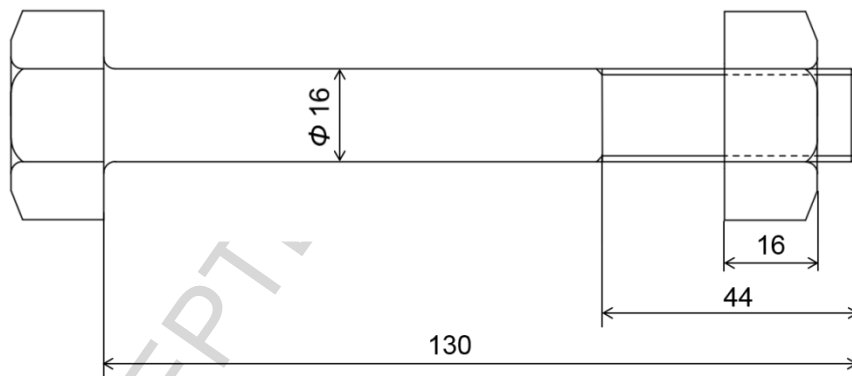


(b) The nut pitch is smaller than the bolt pitch

Fig. 1 Contact status between bolt and nut threads before and after loading (↔ contact)

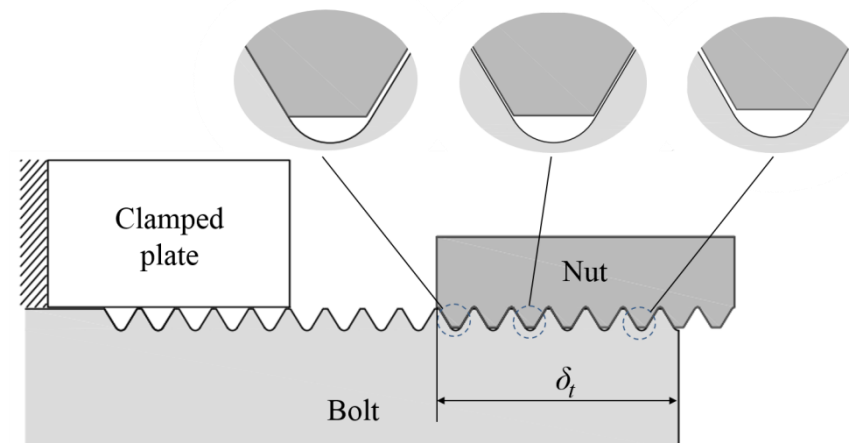


(a) Specimen in loosening experiment

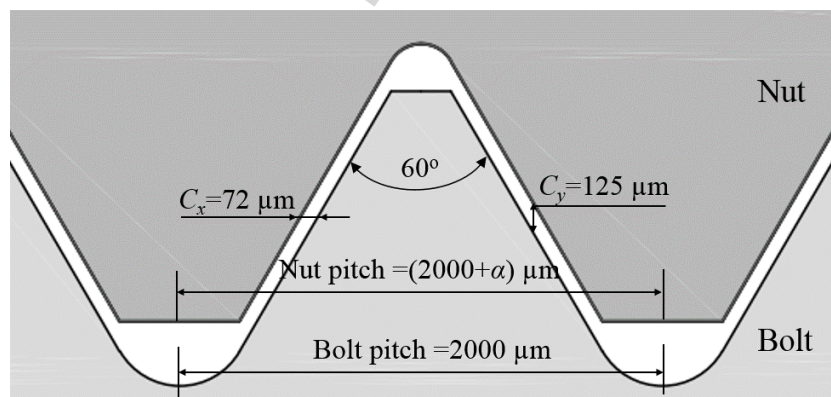


(b) Specimen in fatigue experiment

Fig. 2 Bolt-nut specimen (dimensions in mm)



(a) Contact status between bolt and nut when the nut pitch is slightly larger than the bolt pitch (δ_t : The distance where the prevailing torque appears)



(b) Pitch difference and clearance between bolt and nut

Fig. 3 Schematic illustration of bolt-nut connection having a pitch difference

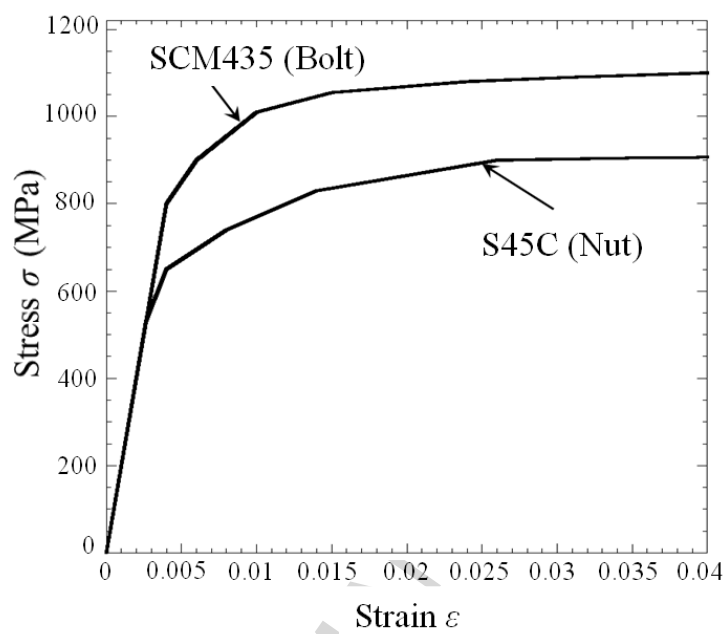


Fig. 4 Stress strain relation for SCM435 (Bolt) and S45C (Nut)

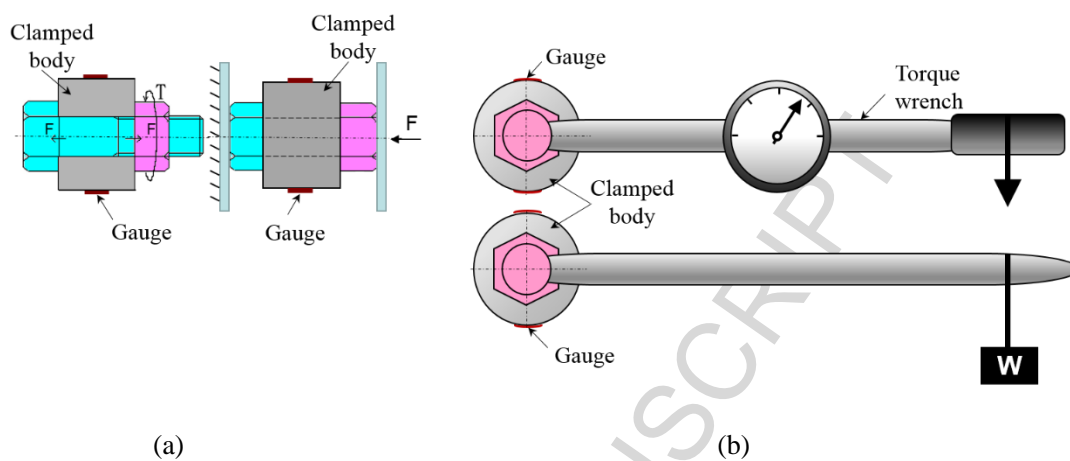


Fig. 5 (a) Calibration method for bolt axial force measurement and (b) Calibration method for torque wrench

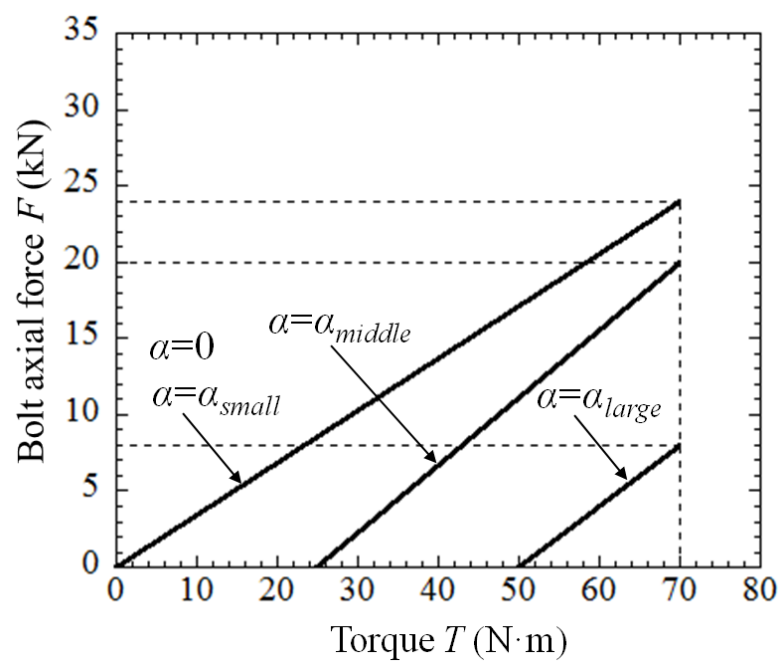


Fig. 6 Relationship between torque and clamping force

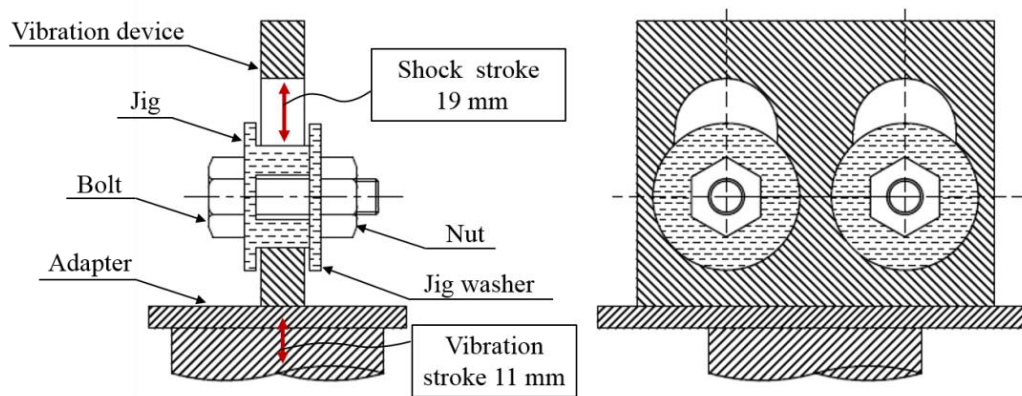
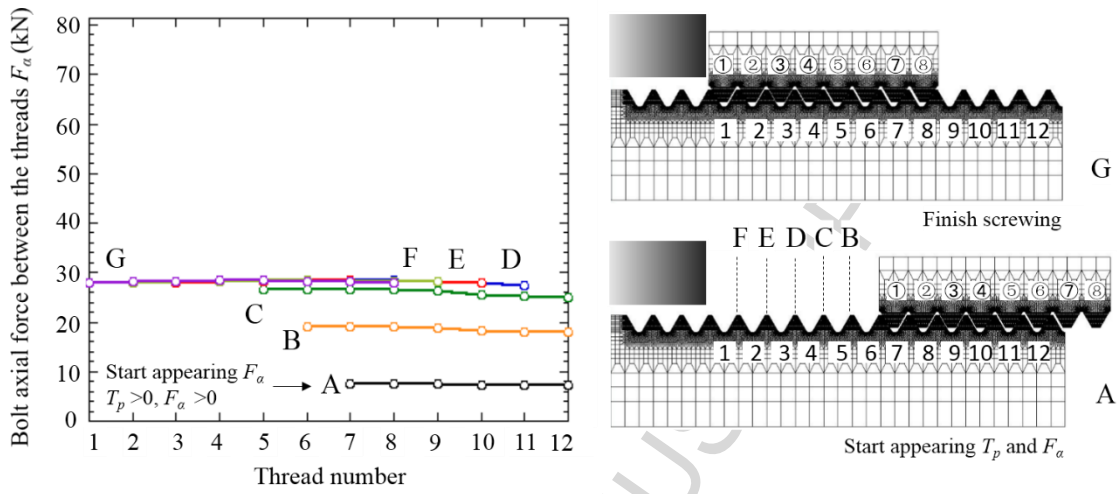
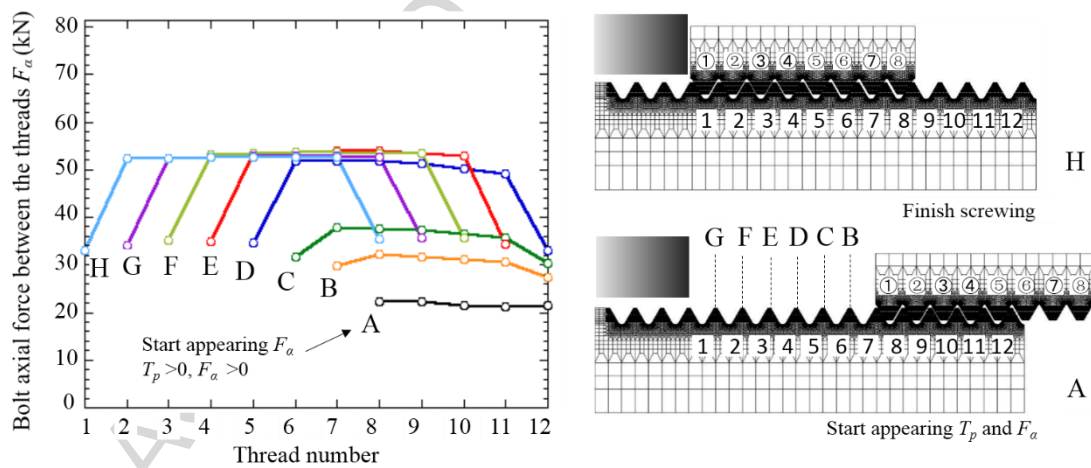


Fig. 7 Loosening experimental device based on NAS3350 (dimensions in mm)

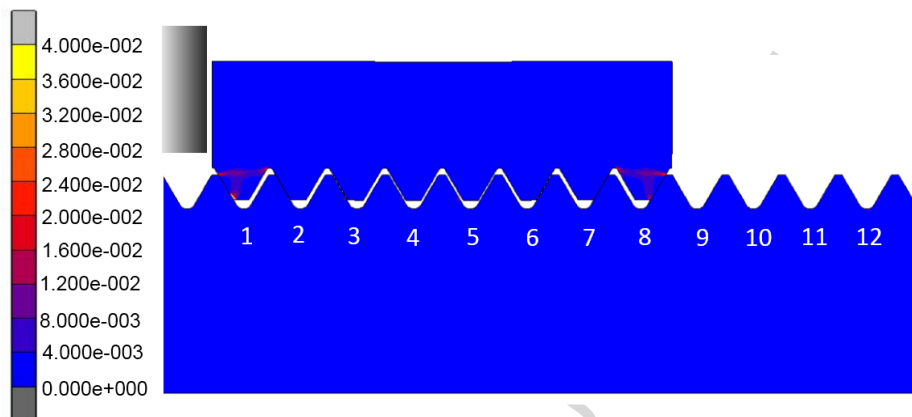


(a) $\alpha = \alpha_{middle}$, from Position A to Position G

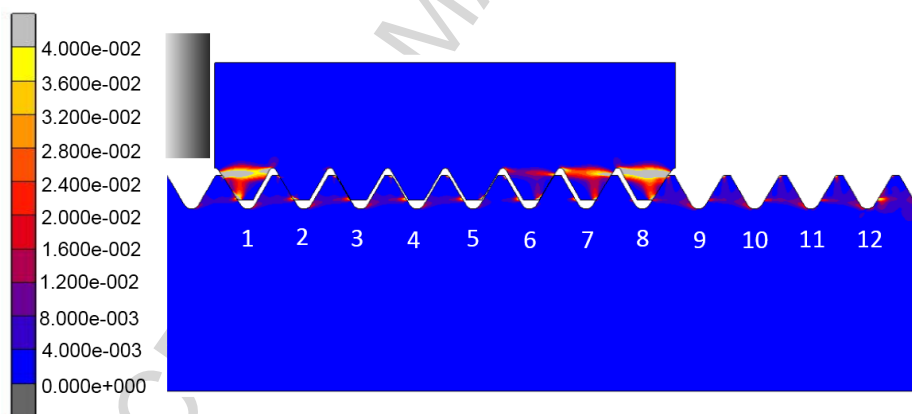


(b) $\alpha = \alpha_{verylarge}$, from Position A to Position H

Fig. 8 Bolt axial force for the screwing process when the bolt is SCM435 and nut is S45C



(a) $\alpha = \alpha_{middle}$, Position G



(b) $\alpha = \alpha_{verylarge}$, Position H

Fig. 9 Equivalent plastic strain when the bolt is SCM435 and nut is S45C

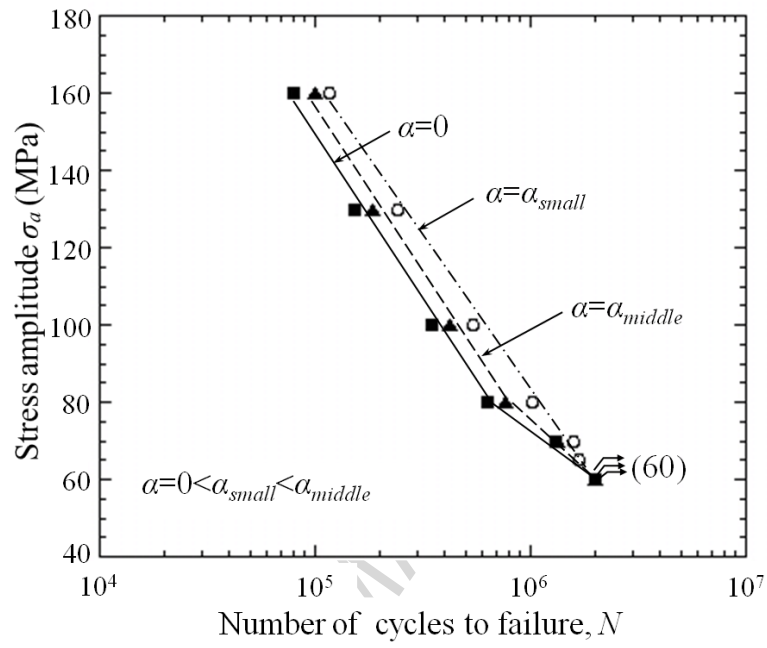


Fig. 10 S-N curves for $\alpha=0$, α_{small} and α_{middle}

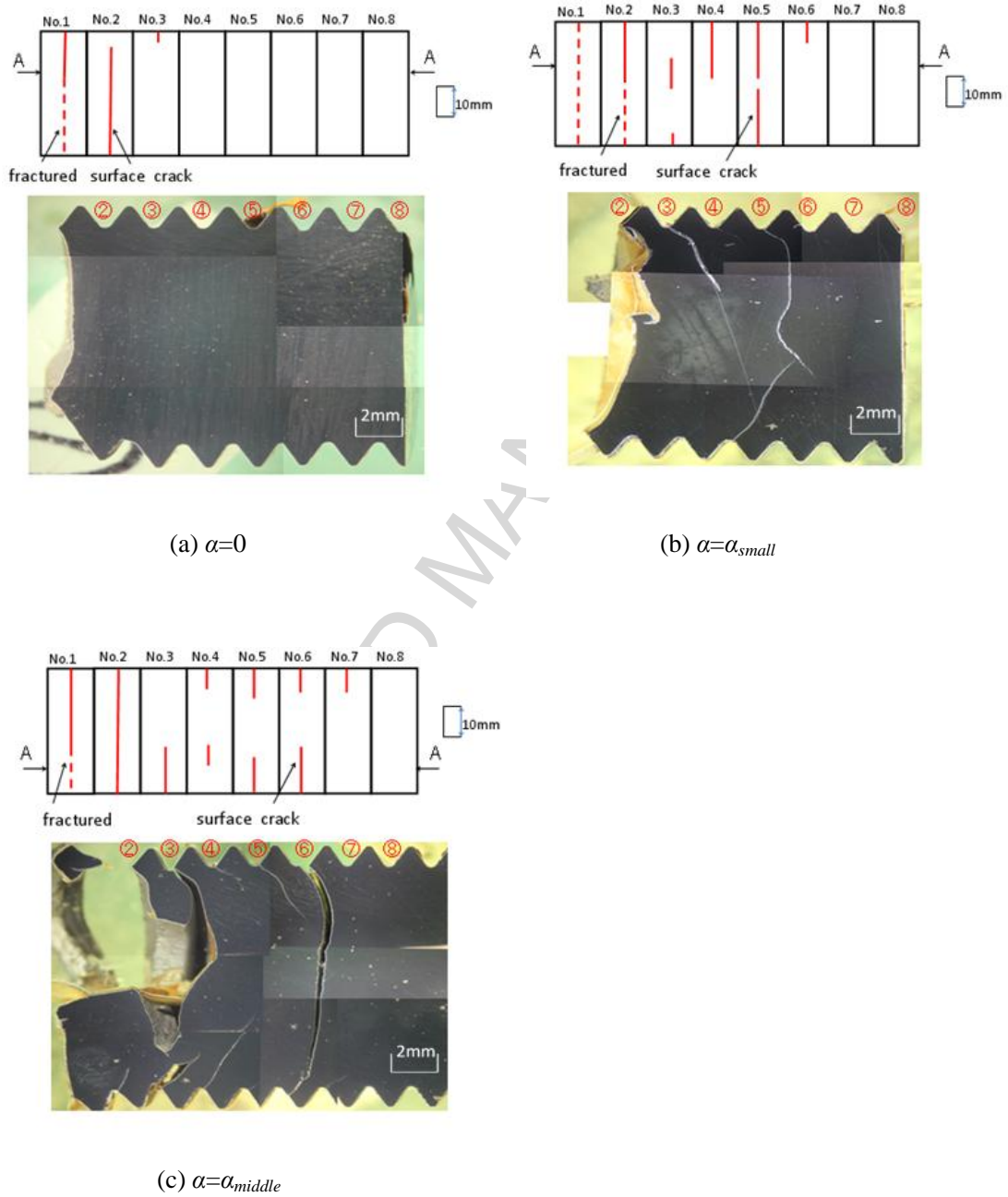


Fig. 11 Observation of crack trajectories ($\sigma_a=100$ MPa, $F=30\pm 14.1$ kN)

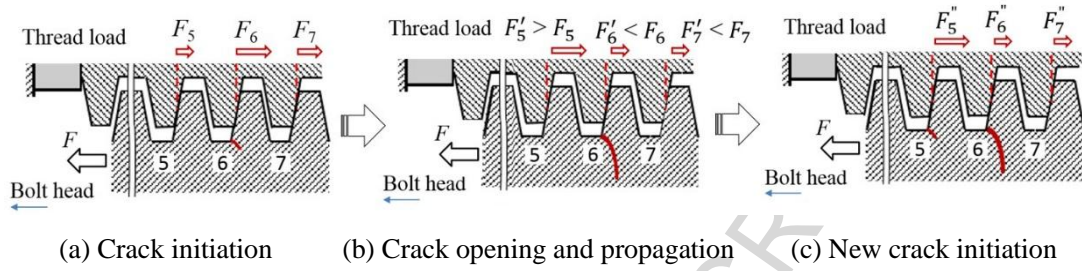


Fig. 12 Crack initiation and extension mechanism due to thread load

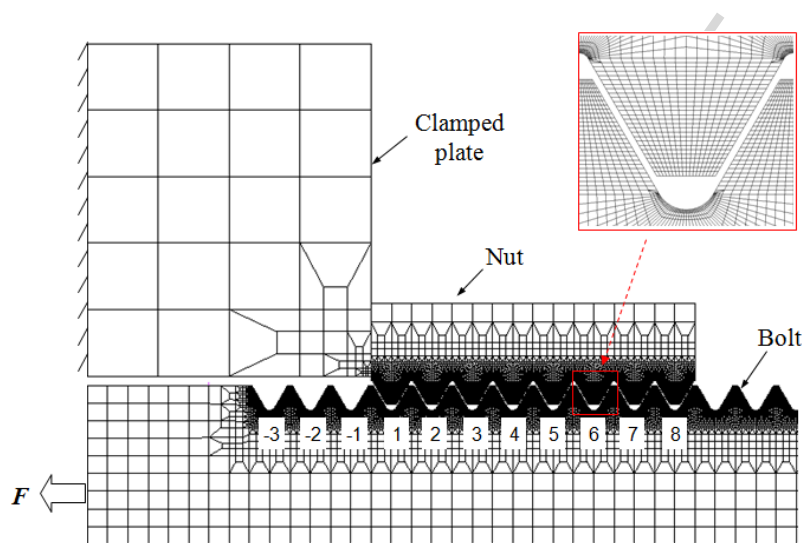
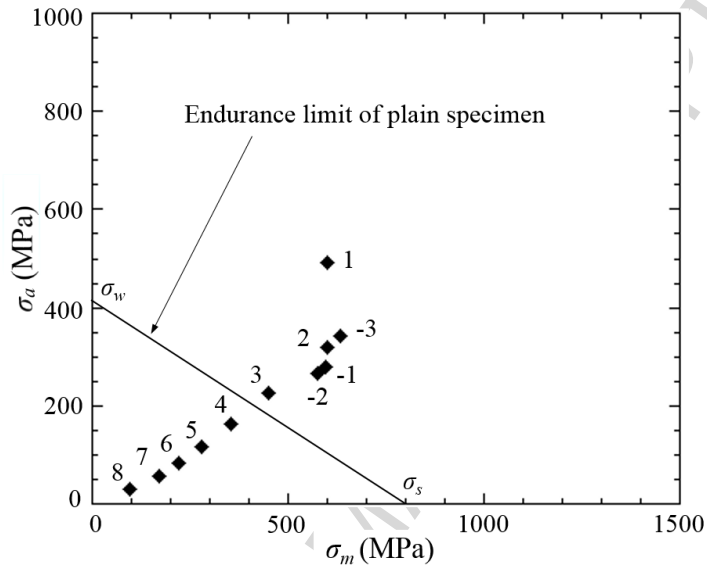
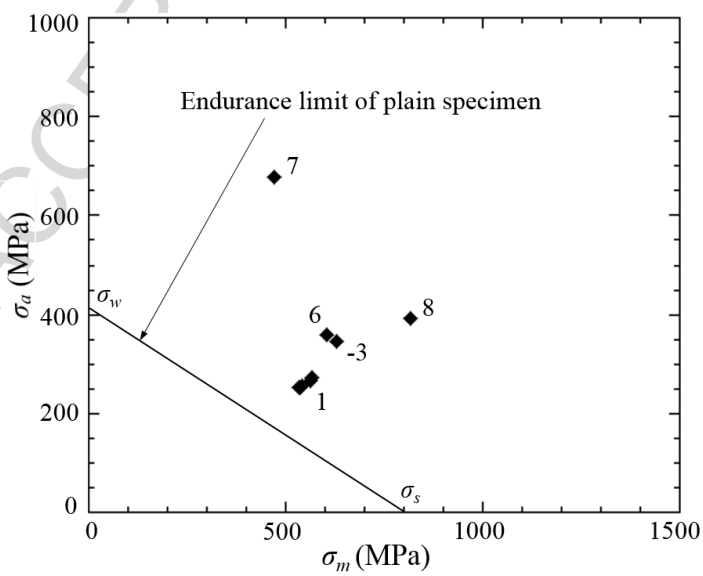
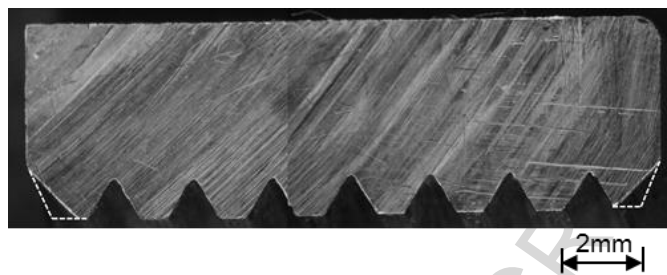
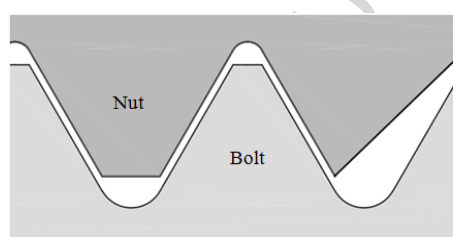


Fig. 13 Axisymmetric finite element model

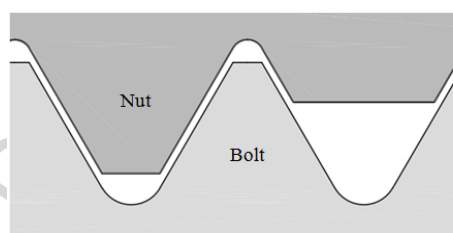
(a) $\alpha=0$ (b) $\alpha=\alpha_{small}$ Fig. 15 Endurance limit diagram ($\sigma_a=100$ MPa)



(a) Incomplete threads at nut ends by cut away

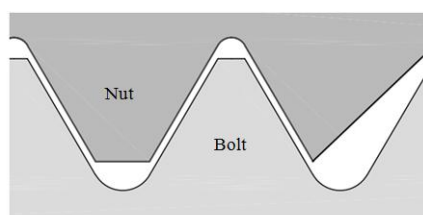


Actual thread

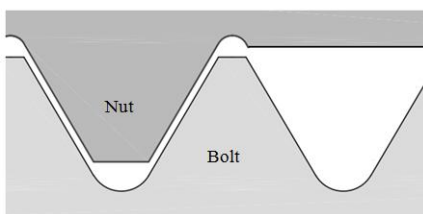


Model A

(b) Incomplete thread model A



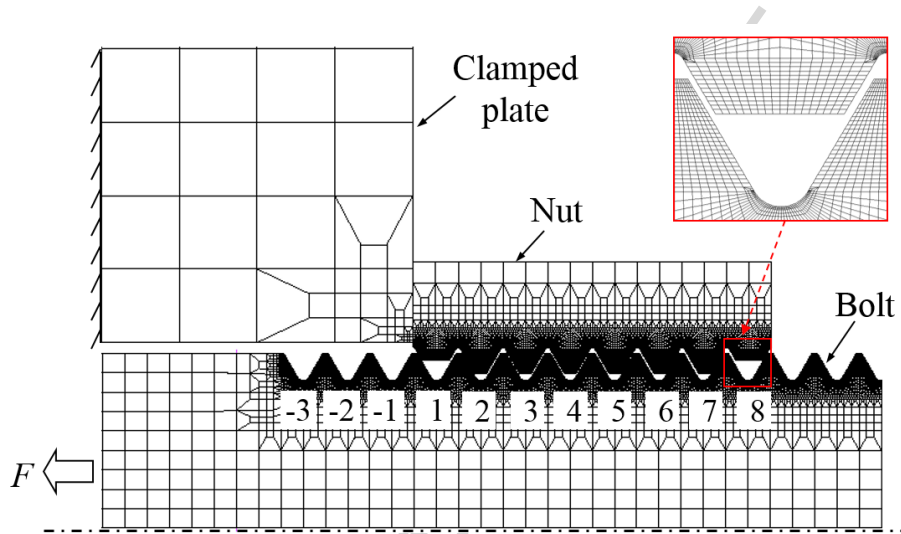
Actual thread



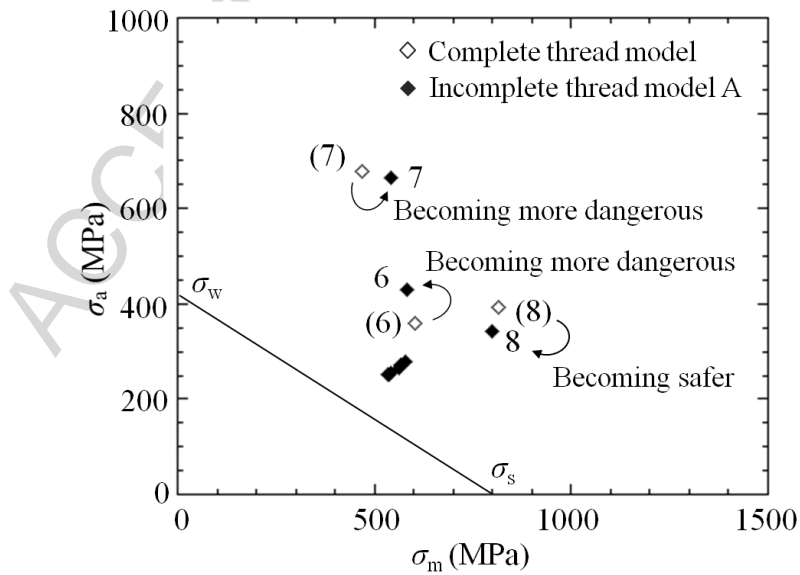
Model B

(c) Incomplete thread model B

Fig. 16 Incomplete threads at nut ends by cut away and incomplete thread models

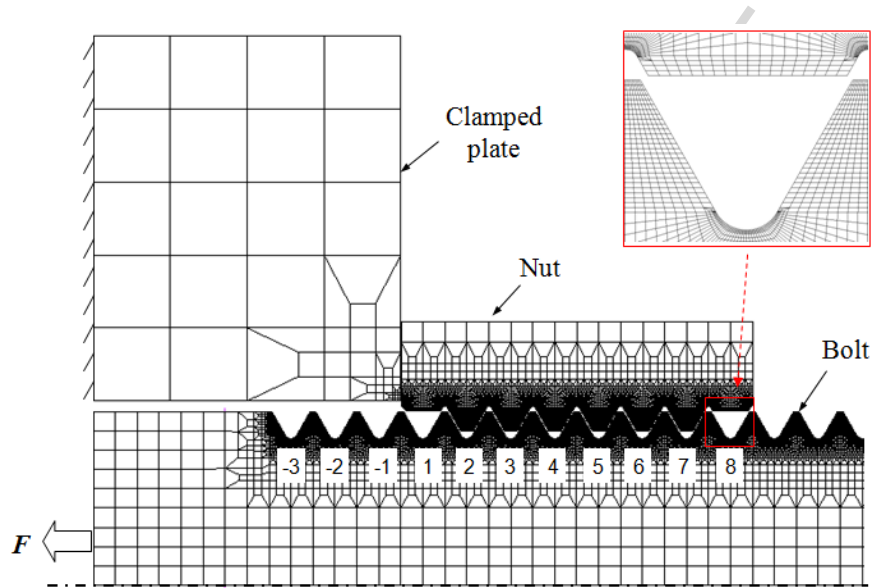


(a) Axisymmetric finite element mesh for model A considering incomplete thread

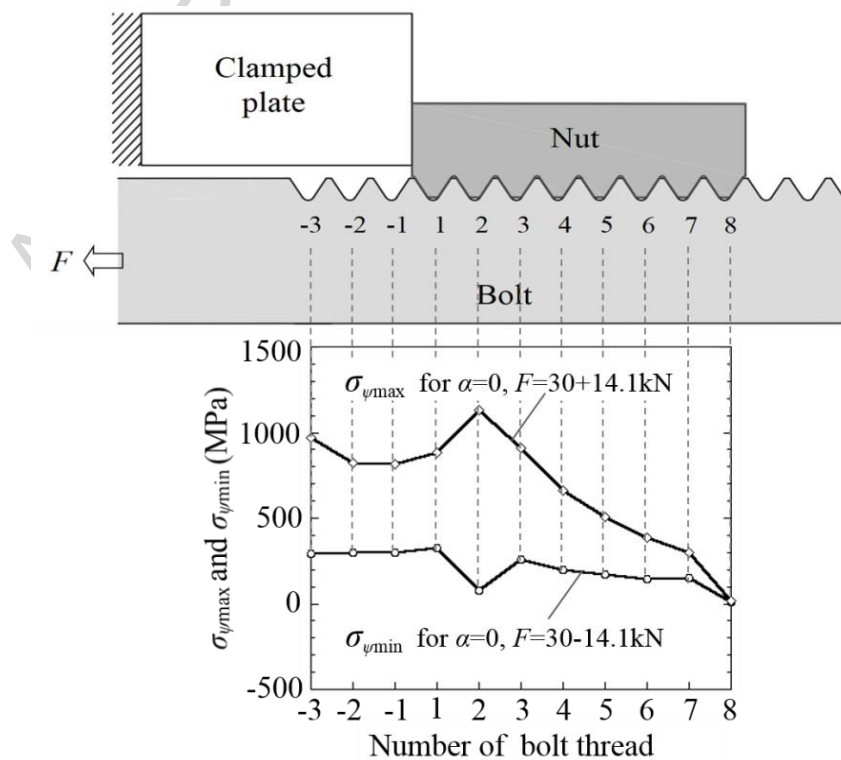


(b) Endurance limit diagram for $\alpha=\alpha_{small}$ when $\sigma_a=100\text{MPa}$, incomplete thread model A vs. complete thread model

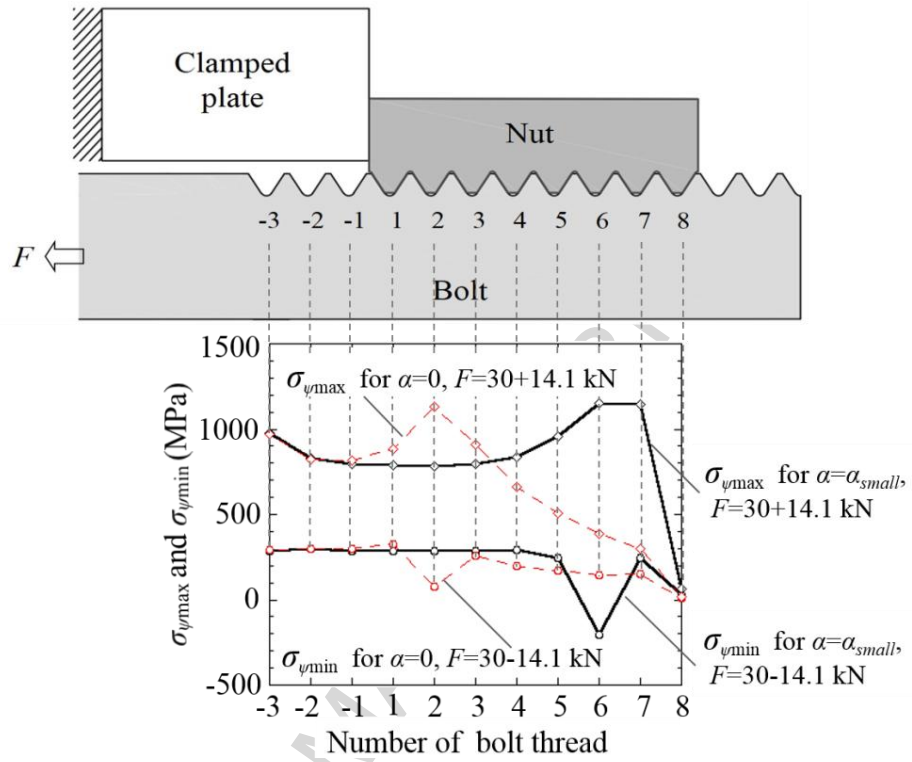
Fig. 17 Axisymmetric finite element mesh for model A considering incomplete thread and analytical result when $\sigma_a=100$ MPa



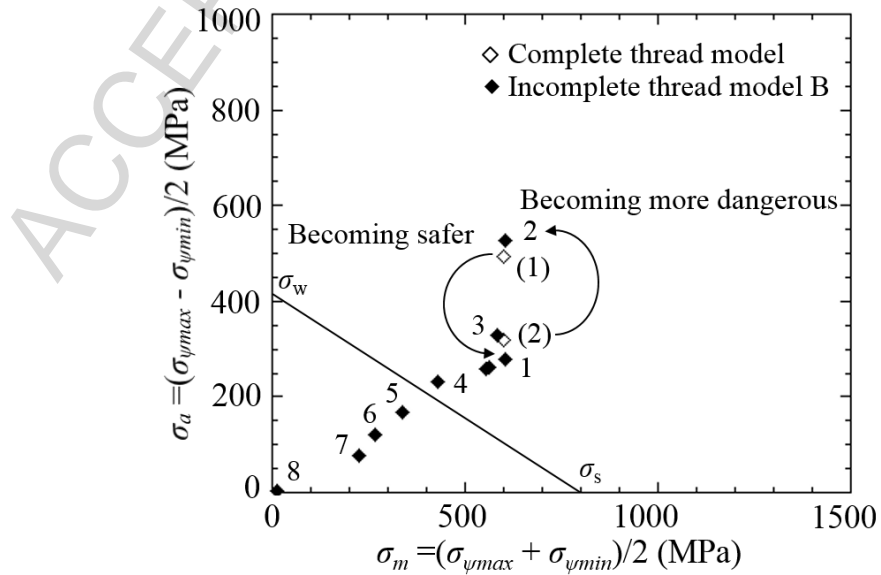
(a) Axisymmetric finite element mesh for model B considering incomplete threads at both ends of nut



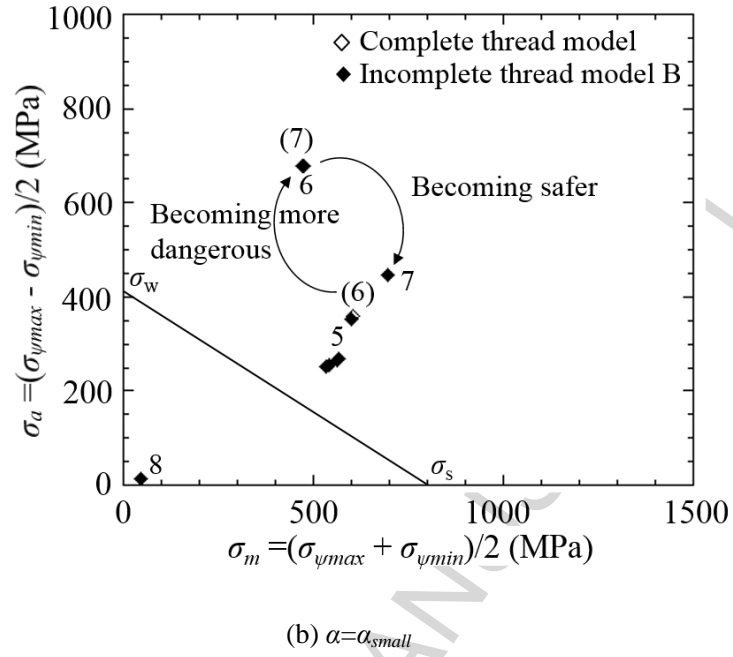
(b) Maximum stress $\sigma_{\psi\max}$ and minimum stress $\sigma_{\psi\min}$ at each thread for model B when $\alpha=0$



(c) Maximum stress $\sigma_{\psi max}$ and minimum stress $\sigma_{\psi min}$ at each thread for model B when $\alpha=\alpha_{small}$



(d) Endurance limit diagram for $\alpha=0$, incomplete thread model B vs. complete thread model



(e) Endurance limit diagram for $\alpha = \alpha_{small}$, incomplete thread model B vs. complete thread model

Fig. 18 Axisymmetric finite element mesh for model B considering incomplete thread and analytical result when $\sigma_a = 100$ MPa

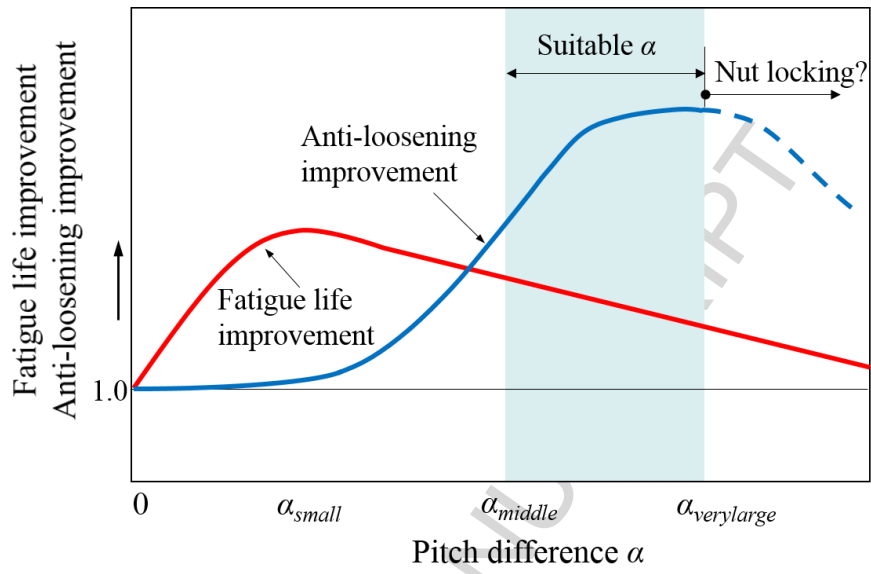


Fig. 19 Schematic illustration of the fatigue life improvement and anti-loosening improvement

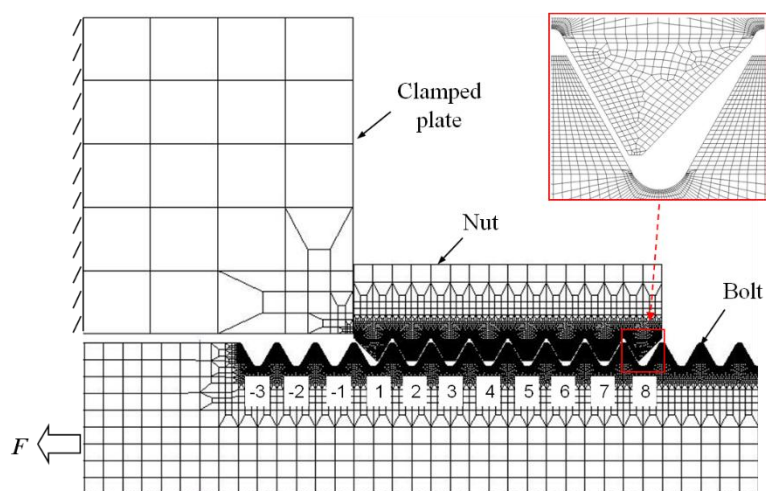


Fig. A1 Axisymmetric finite element mesh for chamfered thread model

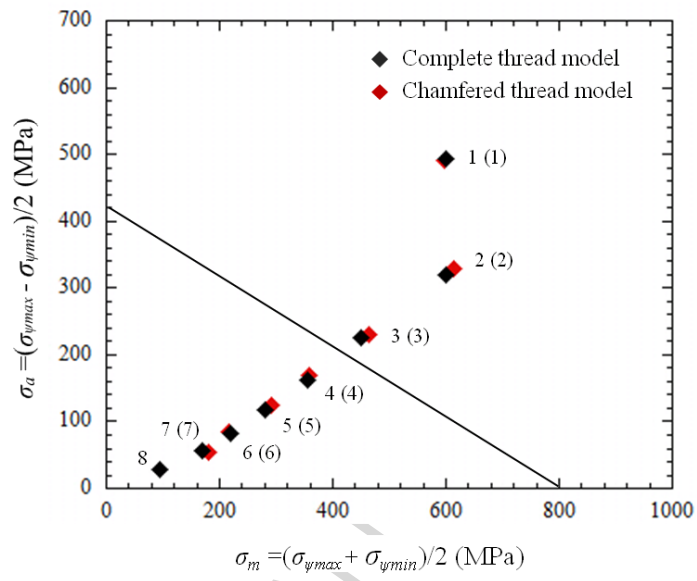


Fig. A2 Comparison between the results of chamfered thread model and complete thread model when $\alpha=0$ and $\sigma_a=100$ MPa

Table Caption List

Tabl	Comparison of some special bolt-nut connections
e 1	
Tabl	Properties of bolt and nut material
e 2	
Tabl	Position where prevailing torque appears, δ_i , and number of nut threads contacted, n_c
e 3	
Tabl	Anti-loosening Performance
e 4	

ACCEPTED MANUSCRIPT

Table 1 Comparison of some special bolt-nut connections

	Anti-loosening performance	Fatigue strength improvement	Machinability	Low cost
This study [24, 25]	◎	○	○	○
CD bolt [8]	△	○	△	△
Super slit nut [4, 5]	○	△	×	×
Hard lock nut [2]	○	△	×	×
Standard bolt-nut	△	○	○	◎

×: bad △: fair ○: pretty ◎: remarkable

Table 2 Properties of bolt and nut material

	Young's modulus (GPa)	Poison's ratio	Yield strength (MPa)	Tensile strength (MPa)
SCM435 (Bolt)	206	0.3	800	1200
S45C (Nut)	206	0.3	530	980

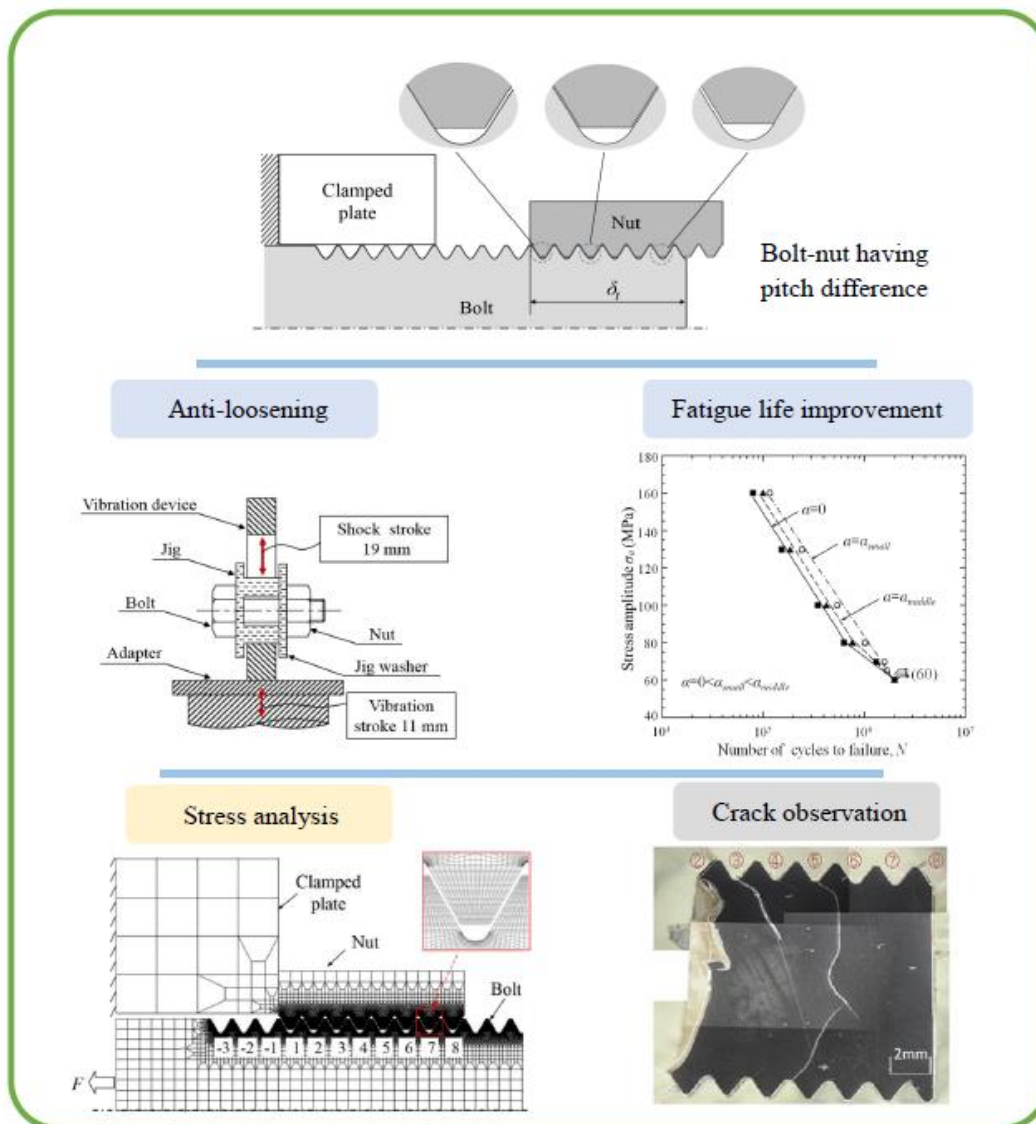
Table 3 Prevailing torque, T_p , contact distance, δ_t , and number of threads in contact (nut), n_c

Pitch difference α	Theoretically obtained δ_t (mm)	The number of nut threads in contact n_c	Prevailing torque T_p (N·m)
0	-	-	No
α_{small}	19.2	9.6 (>8)	No
α_{middle}	8.8	4.4 (<8)	25
α_{large}	7.4	3.7 (<8)	50
$\alpha_{verylarge}$	5.8	2.9 (<8)	Fixed

Table 4 Anti-loosening Performance

Pitch difference α	Sample	Nut drop	Cycles for dropping	Cycles for start loosening	Prevailing torque (N·m)	Axial force* (kN)
0	No.1	Yes	751	-	0	24
	No.2		876	-		
α_{small}	No.3		813	-	0	24
	No.4		1528	-		
α_{middle}	No.5	No	30000	21000	30	20
	No.6		30000	30000		
α_{large}	No.7		30000	30000	67	8
	No.8		30000	30000	57	
$\alpha_{verylarge}$	No.9	-	-	-	>70	-

(*Axial force is estimated from Fig. 6)



Graphical abstract

Highlights

- Bolt-nut with various pitch difference are studied experimentally and analytically.
- A suitable pitch difference can realize the anti-loosening performance.
- A suitable pitch difference can extend the fatigue life to about 1.5 times.
- Pitch difference affects the crack trajectories of bolt significantly.

ACCEPTED MANUSCRIPT